Journal of Hydrology 545 (2017) 212–225

Contents lists available at ScienceDirect

Journal of Hydrology

journal homepage: www.elsevier.com/locate/jhydrol

Research papers

Measurement and modeling of rainfall interception by two differently aged secondary forests in upland eastern Madagascar

Chandra Prasad Ghimire [a,*], L. Adrian Bruijnzeel [b], Maciek W. Lubczynski [a], Maafaka Ravelona [c], Bob W. Zwartendijk [d], H.J. (Ilja) van Meerveld [d]

[a] Faculty of Geo-information and Earth Observation (ITC), University of Twente, Enschede, The Netherlands
[b] Department of Geography, King's College London, London, United Kingdom
[c] Laboratoire des Radio-Isotopes, University of Antananarivo, Antananarivo, Madagascar
[d] Department of Geography, Hydrology and Climate, University of Zurich, Zurich, Switzerland

ARTICLE INFO

Article history:
Received 18 April 2016
Received in revised form 19 October 2016
Accepted 20 October 2016
Available online 20 October 2016

This manuscript was handled by Tim R. McVicar, Editor-in-Chief, with the assistance of Huade Guan, Associate Editor

Keywords:
Forest regeneration
Revised analytical interception model
Secondary tropical forest
Stemflow
Throughfall

ABSTRACT

Secondary forests occupy a larger area than old-growth rain forests in many tropical regions but their hydrological functioning is still poorly understood. In particular, little is known about the various components of evapotranspiration in these possibly vigorously regenerating forests. This paper reports on a comparison of measured and modeled canopy interception losses (*I*) from a semi-mature (ca. 20 years) and a young (5–7 years) secondary forest in the lower montane rain forest zone of eastern Madagascar. Measurements of gross rainfall (*P*), throughfall (Tf), and stemflow (Sf) were made in both forests for one year (October 2014–September 2015) and the revised analytical model of Gash et al. (1995) was tested for the first time in a tropical secondary forest setting. Overall measured Tf, Sf and derived *I* in the semi-mature forest were 71.0%, 1.7% and 27.3% of incident *P*, respectively. Corresponding values for the young forest were 75.8%, 6.2% and 18.0%. The high Sf for the young forest reflects the strongly upward thrusting habit of the branches of the dominant species (*Psiadia altissima*), which favours funneling of *P*. The value of *I* for the semi-mature forest is similar to values reported for old-growth tropical lower montane rain forests elsewhere but *I* for the younger forest is higher than reported for similarly aged tropical lowland forests. These findings can be explained largely by the prevailing low rainfall intensities and the frequent occurrence of small rainfall events. The revised analytical model was able to reproduce measured cumulative *I* at the two sites accurately and succeeded in capturing the variability in *I* associated with the seasonal variability in rainfall intensity, provided that Tf-based values for the average wet-canopy evaporation rates were used instead of values derived with the Penman-Monteith equation.

1. Introduction

Across the tropics, old-growth forest continues to be cleared for grazing, cropping and extractive tree plantations (notably rubber and oil palm; Ziegler et al., 2009a; FAO, 2010; Carlson et al., 2013). However, much of the cleared land is not converted to permanent agricultural use. Land is often abandoned after several years of cultivation, after which natural regrowth may follow. As much as 60% of tropical 'deforestation' has been estimated to occur within the context of swidden cultivation (Geist and Lambin, 2002; Mukul et al., 2016), in which the land is occupied for 1–2 years of cropping and subsequently left to regenerate (Lawrence et al., 2010; Fox et al., 2000, 2009). Further, agricultural land in many tropical upland areas is abandoned as rural peasants move to urban centres (Aide and Grau, 2004; Crk et al., 2009; Lambin and Meyfroidt, 2010) or because the decline in soil fertility makes the land no longer useful for agriculture (Ziegler et al., 2009b). As a consequence, secondary forests are expanding rapidly and nowadays constitute the dominant forest type in many tropical regions (FAO, 2010; Chazdon, 2014). Nevertheless, knowledge of many aspects of the hydrological functioning of tropical secondary forests is severely limited (Bruijnzeel, 2004; Hölscher et al., 2005; Ziegler et al., 2009b; Zimmermann et al., 2013; Mukul and Herbohn, 2016). In particular, little is known about the water use (evapotranspiration) of these often vigorously regenerating forests (Giambelluca, 2002; cf. Mukul et al., 2016). During the first five years of forest succession, vegetation water uptake tends to be (much) less than that of old-growth tropical rain forest (Hölscher et al., 1997) but it has been suggested that soil water uptake after

* Corresponding author at: P.O. Box 217, 7500 AE Enschede, The Netherlands.
E-mail address: c_ghimire@yahoo.com (Chandra Prasad Ghimire).

http://dx.doi.org/10.1016/j.jhydrol.2016.10.032
0022-1694/

the initial stage of regrowth may well be significantly higher than that of old-growth forest, although it is unknown for how long values may remain elevated (Giambelluca et al., 2000; Giambelluca, 2002). Rainfall interception losses from tropical secondary forests have also been shown to generally increase (but not always; e.g. Hölscher et al., 2003) with age of the regrowth (and thus with leaf area) but patterns appear to differ between regions. In some areas (e.g. Panamá) there are indications that interception losses become similar to those of old-growth forest after ca. 10 years of forest recovery (Zimmermann et al., 2013; Macinnis-Ng et al., 2012, 2014). In other areas (e.g. Eastern Amazonia) reported interception values are already similar to those in old-growth forest after less than five years of regrowth (Hölscher et al., 1998; Wickel, 2004; Ubarana, 1996; Roberts et al., 2005), while distinctly higher losses were observed in a 10-year-old stand (Hölscher et al., 1998).

A related issue concerns the fact that significant improvement in top-soil infiltration capacity – and therefore in potential soil- and groundwater recharge – during tropical forest succession may well take 1–2 decades (Ziegler et al., 2004; Zimmermann and Elsenbeer, 2009; Hassler et al., 2011). As stated previously, net precipitation inputs to the soil are typically enhanced during the first 5–10 years of forest succession relative to later growth stages, thereby possibly causing a temporary discrepancy between amounts of water arriving at the forest floor and the capacity of the soil to absorb these during early successional stages (Zimmermann et al., 2013). Therefore, taken together with the possibly enhanced soil water uptake by regenerating forest referred to earlier, a negative overall effect of tropical forest regrowth on streamflow regime can, therefore, not be excluded (Lacombe et al., 2015).

The eastern uplands of Madagascar provide a case in point: forests in the area have been cut, burned and used for subsistence agriculture for many decades but increasingly so in recent years (Styger et al., 2007). Little is known quantitatively about how this intensifying land use and the presence of vegetation in various stages of regrowth dotted across the landscape affect local hydrological processes and streamflow regimes (e.g. Bailly et al., 1974) but understanding the underlying mechanisms and processes is critical in view of the area's seasonal climate. This work is part of a larger study that investigates the various environmental services of different types of land use and land cover in eastern Madagascar – including a possible negative 'trade-off' between potentially enhanced evapotranspiration losses from regenerating forest versus likely improved infiltration conditions compared to degraded fire-climax grassland (baseline situation). The objectives of this paper were thus to: (i) analyse rainfall interception losses from a semi-mature (ca. 20-year-old) and a young (5–7 years old) secondary forest in the lower montane rain forest belt of eastern Madagascar, and (ii) shed light on the causes underlying any contrasts in rainfall interception between the two forests. In order to do so, throughfall and stemflow were measured over a one-year period at both sites while a physically-based interception model (Gash et al., 1995) was applied for the first time in a tropical secondary forest setting to explore the relative importance of climatic and forest structural factors to overall interception loss.

2. Study area

The study was conducted within the Ankeniheny-Zhamena corridor (CAZ) in eastern Madagascar. The CAZ is a newly protected area that encompasses one of the largest remaining blocks of rain forest in Madagascar (Fig. 1) and is home to ca. 350,000 people and many endemic species (Conservation International, 2011; Portela et al., 2012). Depending on elevation, the rain forest is classified as evergreen humid forest of low elevation (0–800 m) or mid-elevation (800–1800 m). Metamorphic and igneous rocks form the dominant geological substrate in which highly leached Ferralsols have developed (Du Puy and Moat, 1996). Over the past century, much of the rain forest of eastern Madagascar has disappeared. The main threat to the remaining forests is the long-practiced slash-and-burn agricultural system (Styger et al., 2007). Upland rice is cultivated usually for one season, followed by a root crop during the next season, after which the land is abandoned to allow natural regrowth and soil fertility recovery before being used again for agricultural cropping after ca. 15 years (fallow cycle). However, in recent decades, fallow periods have shortened to as little as 3–5 years due to increased population pressure, which has led to declining crop yields and increased pressure on the remaining forests and regenerating vegetation (Styger et al., 2007; Portela et al., 2012). This has resulted in a highly fragmented landscape composed of rain forest remnants, secondary forests at various stages of regrowth and young fallow vegetation on abandoned land, as well as fire-climax grassland, scattered agricultural fields and rural villages.

The CAZ experiences a tropical monsoon climate (Köppen-type Am). Depending on elevation and exposure to moist oceanic air masses, the average annual precipitation within the CAZ varies between 1000 and 4000 mm (1983–2013; Météo Madagascar, 2013). Mean (± standard deviation, SD) annual rainfall measured in Andasibe at mid-elevation (990 m.a.s.l.) for the 1983–2013 period was 1625 (± 260) mm (Météo Madagascar, 2013). The region is characterized by two seasons: a hot, rainy season from November to April and a cooler, dry season from May to October. The rainy season brings about 75% of the total annual rainfall. In general, September is the driest month with only 2% of the annual total precipitation. The wettest months are January and February, together accounting for about 36% of the average annual rainfall (Météo Madagascar, 2013). Average monthly temperatures at Andasibe range from 15 °C in July to 22 °C in December. The average monthly relative humidity as measured between October 2014 and November 2015 varied from 85% in October to 94% in July. Occasionally strong winds and heavy rainfall are common during the November to May cyclone season (Tadross et al., 2008) but average monthly wind speeds are less than 2 m s^{-1}.

The measurements for this study were carried out in two 0.25 ha forest plots situated in the mid-montane forest zone (Du Puy and Moat, 1996): a semi-mature (ca. 20 years old) secondary forest (SMF) and a young secondary forest (YSF, 5–7 years old). Note that mid-montane forests in Eastern Madagascar would classify as lower montane rain forests in the widely used tropical forest classification scheme of Grubb (1977). The two plots are located near Andasibe, ca. 2500 m apart on fairly steep slopes (15–20°) underlain by gneissic rocks (Table 1). The SMF plot is located on a northeast-facing slope at ~950 m.a.s.l. and the YSF on a northwest-facing slope at ~990 m.a.s.l.

The evergreen SMF had mostly re-sprouted after repeated illegal manual logging ceased in 1995. The site was never fully cleared, burned or cultivated and is now a protected forest managed by a local NGO. The vast majority of the trees were ~20 years old at the time of the measurements with ~65% of all trees with a diameter at breast height (DBH) ⩾ 5 cm belonging to the 5–10 cm diameter class and 33% in the 10–20 cm class. Only 1.3% of the trees had a DBH > 20 cm but given the very narrow diameter range observed for this group (21–22 cm) it is unlikely that these represented remnant individuals from the original forest. We classified the SMF as semi-mature because of the intermediate height of the main canopy (~19 m, Table 1) relative to values usually observed for tropical lower montane rain forests (Scatena et al., 2010), the intermediate age (established on the basis of interviews with knowledgeable local informers) and the species richness of the site. The SMF plot had a well-developed understory and contained 72 species; the six dominant tree species *Abarahamia*

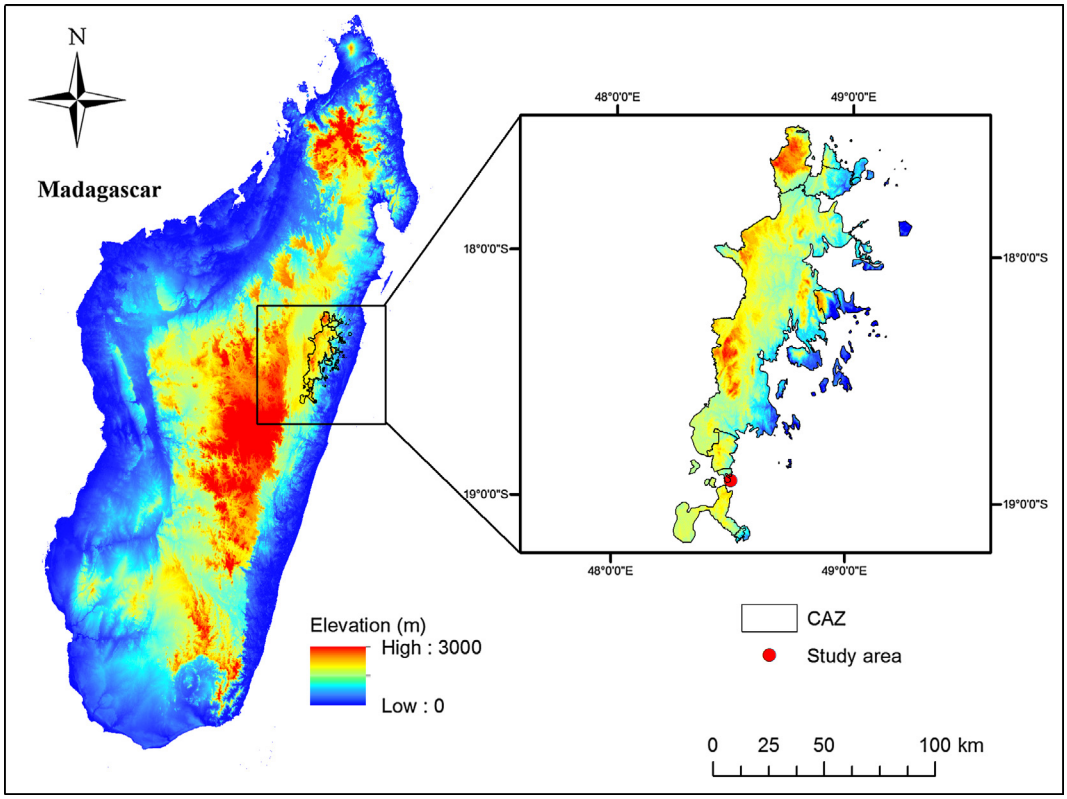

Fig. 1. Location of the study sites in the Ankeniheny-Zhamena corridor (CAZ) in eastern Madagascar.

Table 1
Characteristics of the semi-mature secondary forest (SMF) and the young secondary forest (YSF) study plots.

	SMF	YSF
Elevation (m.a.s.l.)	950	990
Latitude (S)	18.93167°	18.94722°
Longitude (E)	48.41167°	48.39527°
Plot size (m^2)	2500	2500
Aspect	NE	NW
Slope	18°	16°
Average (±SD) DBH (cm)	9.3 (±4.0)	6.1 (±1.3)
Basal area (m^2 ha^{-1})	35.5	6.3
Stem density (stems ha^{-1})	5233	2133
Average (±SD) canopy height (m)	19 (±8.0)	5 (±0.31)
Average (range) LAI (m^2 m^{-2})	3.39 (3.11–3.58)	1.83 (1.75–2.14)

ditimena, *Brachulaena ramiflora*, *Cryptocaria* sp., *Ocotea samosa*, *Eugenia* spp., and *Leptolaena* together comprised 35% of overall stem density. Although evergreen, the SMF canopy shed a small proportion of its leaves towards the end of the dry season. However, the leaf area index (LAI, determined using a Licor LAI 2000 Plant Canopy Analyzer) recovered fairly quickly after the onset of the rainy season. Stand LAI varied from 3.11 (± 0.11) in September 2014 (i.e., the end of the dry season) through 3.39 (± 0.19) in January and 3.58 (± 0.14) in May 2015.

The young secondary forest (YSF) site had primary forest before it was cut and burned for rice cultivation in 1990. The site underwent slash-and-burn agriculture for ca. 10 years, involving three fallow cycles. There has been no slash-and-burn cultivation at this site since 2000, when a forest restoration programme was initiated. The evergreen YSF is primarily composed of *Psiadia altissima* trees (95% of overall stem density) with *Cassinopsis madagascariensis* and *Harungana madagascariensis* together occupying less than 5% of overall stem density. Although the forest restoration programme attempted to introduce various other native species, these were outcompeted by *P. altissima* and did not survive for more than a few years, largely due to a lack of regular follow-up management (particularly the removal of invasive species and other weeds). At the time of the study, the dominant trees in the YSF were ~6 years old with an average canopy height of 5 m (Table 1). The understory was dominated by *Rubus molluccanus*, *Lantana camara* and *Clidemia hirta*. Like the SMF, the YSF canopy also shed a small proportion of its leaves towards the end of the dry season and new leaves emerged quickly after the return of the rain. The LAI of the YSF was 1.75 (± 0.18) in September 2014, 1.83 (± 0.18) in January and 2.14 (± 0.26) in May 2015.

3. Methods

3.1. Field measurements

Rainfall and throughfall were measured at the SMF and YSF plots from 1 October 2014 until 30 September 2015. Gross rainfall (P, mm) was measured for each forest plot in a nearby clearing (ca. 20 m distance for the YSF site and 100 m for the SMF site) using a tipping bucket rain gauge (Rain Collector II, Davis Instruments, USA) connected to a HOBO event logger (Onset Computer Corporation, USA), and a manual rain gauge (CM1016 Skyview, UK; 10 cm orifice diameter) that was used primarily to check the recording gauge. The manual gauges were read daily around 9:00 AM local time. The orifices of all rain gauges were placed at ~1 m above the ground to avoid ground-splash effects. Based on manual calibrations, the tipping bucket gauge at the SMF had a resolution of 0.20 mm per tip, while that at the YSF had a resolution of 0.21 mm per tip. Single tips were not included in our evaluation of rainfall characteristics (because of the unknown duration they represented) but the associated amount at either site was small

(~0.5% of the annual total). Rainfall amounts associated with wind speeds that would be large enough to significantly affect the catch (>5 m s^{-1}; cf. Nespor and Sevruk, 1999) made up only 0.6% of the total during the study period while the average (±SD) wind speed during rainfall was low (0.6 ± 0.65 m s^{-1}). Therefore, wind-induced errors in measured rainfall totals were assumed to be negligible.

A systematic sampling approach was used for the throughfall measurement (Tf, mm). This ensured an even spread of sampling locations and was implemented by dividing the 0.25 ha plots into 50 rectangular sub-plots of 5 m × 10 m each. A funnel-type gauge was positioned in the corners of each subplot, which resulted in 66 gauges in a non-roving arrangement (Fig. 2). The funnel-type gauge consisted of a 5 L collector and a funnel (145 cm^2 orifice area). The orifices of the gauges were positioned 50 cm above the forest floor to avoid splash-in from the ground. The funnel-type gauges were read daily around the same time as the manual rain gauge in the clearing. Measured Tf volumes were converted to equivalent water depth (in mm) by dividing the volume of water in each gauge by the orifice area. The performance of the funnel-type gauges was assessed by regressing the catch of one such gauge (y, mm) placed in the clearing at the YSF site against corresponding amounts collected by the tipping-bucket rain gauge (x, mm). The correlation between the two measurements was strong ($y = 1.05 * x$; $r^2 = 0.99$, $n = 30$) and the relationship was subsequently used to correct the catch of the funnel-type gauges placed beneath the forest canopy. In addition, Tf was measured continuously using three V-shaped stainless steel gutters (200 cm × 30 cm × 15 cm each) per forest plot. The three gutters were uniformly distributed along a diagonal of the 0.25 ha plot (Fig. 2). The gutters were placed at ca. 1 m above the forest floor to avoid splash-in from the ground and at an angle of 25–30° to the horizontal to encourage rapid drainage. Losses by splash from the gutter system were minimized by the V-shaped nature of the sides of the gutter. Each gutter was equipped with a tipping bucket (50 ml per tip) and data-logger device (HOBO event logger, Onset Computer Corporation, USA). The drainage slot at the end of each gutter was covered by a metal mesh to minimize entry of organic debris. Moreover, the gutters were cleaned daily and treated regularly with a silicon solution to prevent blockage by organic material and to minimize wetting losses during drainage, respectively. Tf volumes measured by the gutters were also converted to equivalent water depths (in mm) by dividing water volumes by gutter area (corrected for gutter inclination). Finally, the Tf values from the gutters and the manual gauges were averaged using a weighting procedure that took the relative surface areas of the two types of gauges into account as follows:

$$Tf = \frac{Tf_1 \times A_1 + Tf_2 \times A_2}{A_1 + A_2} \quad (1)$$

where Tf is the weighted average throughfall (mm) per unit ground area and Tf_1 and Tf_2 are the average throughfall amounts (mm) measured with the three gutters and the 66 funnel-type gauges with corresponding total surface areas A_1 and A_2, respectively.

Stemflow (Sf, mm) was measured on five trees in the YSF and on ten trees in the SMF. The selected trees represented the DBH (diameter at breast height) range and dominant species in the plots. Spiral collar gauges were installed at ~1 m from the ground using plastic tubing that was slit open along the length and nailed tightly to the stem. Gaps between stem and tubing were closed using silicon sealant. In the case of species with a loose or rough bark, the bark was shaved prior to installation of the tubing. Each collar was connected to a 20 L collector. The volume of water in the stemflow collectors was measured daily at the same time as the throughfall collectors. Stemflow proved to be only a minor component of the wet-canopy water balance in the SMF, although the number of sampled trees was insufficient to derive a meaningful relationship between Sf and tree DBH for upscaling to the stand level (cf. Manfroi et al., 2004; Holwerda et al., 2006). The monitored trees in the YSF were all of similar size so that we could not obtain a clear relationship between Sf and DBH for the YSF either. For this reason, Sf measurements were scaled up to the plot level by multiplying the average volume per tree species with their corresponding number in the plot. Next, the plot-scale stemflow volume obtained in this way was divided by the plot area (corrected for slope gradient) to derive Sf in mm per unit ground area. Stemflow measurements were carried out from 15 February 2015 until 30 September 2015. The respective average values per forest plot derived for this period (expressed as a fraction of gross rainfall *P*) were used to estimate Sf for the preceding period when stemflow was not measured (i.e. October 2014–January 2015).

Air temperature, relative humidity and wind speed were measured at both sites. At the YSF, the measurements were made at a height of 2 m above the forest canopy using a 7 m mast. It was not feasible to erect a tower that was taller than the canopy in the SMF, largely due to the high stem density and the uneven height distribution of the canopy surface. Therefore, measurements were made using a 10 m mast placed in the nearby clearing where rainfall was measured. At both locations, air temperature (*T*, °C) and humidity (RH, percentage of saturation) were measured using Skye sensors (Skye Instruments Ltd., UK) protected against direct sunlight and precipitation by a radiation shield. Wind speed (m s^{-1}) was measured using an A100R digital anemometer (Vector Instruments, UK). All measurements were taken every 30 s, and 10-min averages were recorded by DataHog2 loggers (Skye Instruments Ltd., UK).

Meteorological data were also acquired by an automatic weather station located in a nearby fire-climax grassland at 965 m.a.s.l. (ca. 1000 m from the SMF site and 1500 m from the YSF site). Incoming short-wave radiation was measured using a CM6B-pyranometer (Kipp and Zonen, The Netherlands), while air temperature (*T*, °C), relative humidity (RH, %), wind speed (m s^{-1}) and wind direction were measured using a Vaisala WXT520 Weather Transmitter (Vaisala Oyj, Finland). All measurements were taken every 30 s, and 5-min averages were recorded by a Campbell Scientific Ltd. CR1000 data-logger. Because of the proximity to the SMF and YSF plots, the incoming short-wave radiation

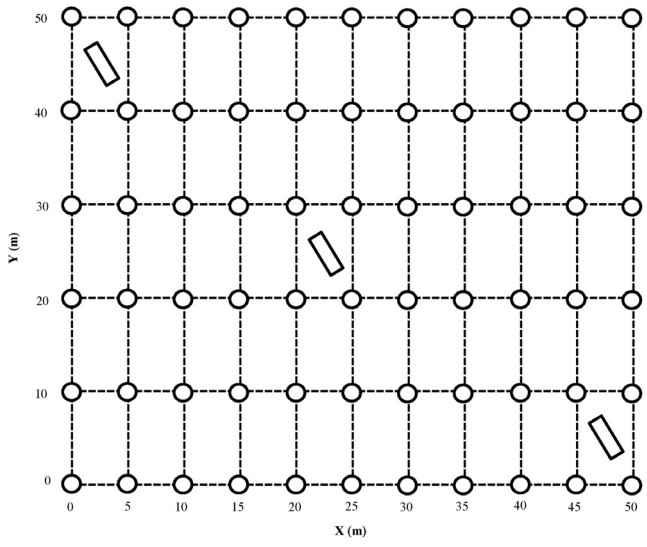

Fig. 2. Sketch of the 0.25 ha throughfall sampling grid used at the semi-mature (SMF) and young secondary (YSF) forest sites. The circles and solid rectangles indicate the positions of funnel-type collectors and recording gutters, respectively.

as recorded in the fire-climax grassland was considered to be the same as that for the two forest plots (see also Section 3.2.2.2 below).

3.2. Rainfall interception model

3.2.1. The revised analytical model for predicting interception loss from sparse vegetation

Rainfall interception loss (I, mm) was determined as the difference between gross and net precipitation, i.e. $P - (\mathrm{Tf} + \mathrm{Sf})$. The revised version of the analytical model of rainfall interception (Gash et al., 1995) was used to model interception losses at the SMF and YSF plots. The revised model takes the sparseness of the canopy into consideration by scaling the average evaporation rate during a rain event (hereafter referred to as wet-canopy evaporation rate; $\bar{E}$, mm h^{-1}) and the canopy storage capacity (S, mm) to the proportion of canopy cover (c) (see Gash et al. (1995) for a full description). The model assumes rainfall to be intercepted during a series of discrete rainfall events with sufficient time between the events for the canopy and the tree trunks to dry. Rainfall events were defined as periods with at least 0.40 mm (SMF) or 0.42 mm (YSF) of rain, separated by a dry period of at least 3 h (cf. Schellekens et al., 1999). Each event of sufficient magnitude to fully wet the canopy consists of up to three sequential phases: (i) a wetting-up phase during which gross rainfall (P) is less than the threshold value required to saturate the canopy (P'_g, mm), (ii) a saturation phase, during which the average rainfall intensity ($\bar{R}$, mm h^{-1}) exceeds the average evaporation rate from the fully wetted canopy, and (iii) a drying phase after rainfall has ceased. Table 2 summarises the respective equations as used in the revised analytical model to calculate the overall interception loss.

The storage of water in the canopy is described using the canopy storage capacity S, which is defined as the amount of water left in a saturated canopy in the absence of evaporation, after rainfall and canopy drainage have ceased (Gash and Morton, 1978). S is the product of the canopy storage capacity per unit area of cover S_c and the canopy cover fraction, c. The free throughfall coefficient, p (here assumed to be equal to $1 - c$), is the proportion of incident rainfall that falls directly on the forest floor without hitting the canopy. Evaporation from the tree trunks is specified in terms of trunk storage capacity (S_t, mm) and the proportion of rain that is diverted to stemflow (p_t). Similarly, the wet-canopy evaporation rate per unit area of land ($\bar{E}$) during rainfall is scaled to the proportion of the canopy cover to obtain the evaporation rate per unit area of cover, $\bar{E}_c$. Rainfall rates $\geqslant 0.5$ mm h^{-1} are generally assumed to be sufficient to maintain saturated canopy conditions (Gash, 1979; Schellekens et al., 1999). The amount of water needed to saturate the canopy (P'_g, mm) is calculated using Eq. (2) (Gash et al., 1995):

$$P'_g = -\frac{\bar{R}}{\bar{E}_c} S_c \ln\left(1 - \frac{\bar{E}_c}{\bar{R}}\right) \quad (2)$$

Table 2
The equations describing the five components of rainfall interception in the revised analytical model (after Gash et al., 1995). See text for explanation.

Component of interception loss	Formula
m small storms insufficient to saturate the canopy ($P < P'_g$)	$c\sum_{j=1}^{m} P_j$
Wetting up the canopy in n large storms ($P \geqslant P'_g$)	$ncP'_g - ncS_c$
Evaporation from saturated canopy until throughfall ceases	$\left(c\frac{\bar{E}_c}{\bar{R}}\right)\sum_{j=1}^{n}\left(P_j - P'_g\right)$
Evaporation after throughfall has ceased	ncS_c
Evaporation from trunks; q storms with $P > S_t/p_t$, which saturate the canopy	$qS_t + p_t\sum_{j=1}^{n-q} P_j$

For each site, the rainfall data were divided into two sub-sets: sub-set 1 for model calibration and sub-set 2 for model validation. To account for seasonal variation in rainfall intensity, the data from November, January, February, May and June were used for model calibration and the data from October, December, March, April, May, July and September for model validation. Since the validation data-set was not used for the derivation of the canopy structural parameters (p, S, p_t and S_t), this procedure ensured an independent validation. Because there was typically one rainfall event per day (both at the SMF and YSF), daily rainfall and interception loss data were used in the modeling (see below).

3.2.2. Derivation of the model parameters

3.2.2.1. Canopy structural parameters. The canopy storage capacity (S) was estimated from measurements of gross rainfall (P) and throughfall (Tf), following Jackson (1975). This method also allows the derivation of the free throughfall coefficient (p) from the slope of the regression between P and Tf for events that are too small to saturate the canopy (i.e. $<P'_g$). It is assumed that evaporation losses during these small events are negligible. In the Jackson (1975) approach, S is determined as:

$$S = P_i - \mathrm{Tf}_i \quad (3)$$

where the subscript i denotes the knickpoint in the P vs Tf graph at the point where drainage from the canopy starts to contribute to direct Tf. The two stemflow-related parameters S_t and p_t, were derived following the method of Gash and Morton (1978) as the negative intercept and the slope of the linear regression between Sf and P, respectively. Vegetation parameters may vary seasonally in response to changes in LAI (Van Dijk and Bruijnzeel, 2001a,b) but the observed variation in LAI, in combination with the low rainfall amounts during the dry season (~20%), proved too small to have a significant effect on overall interception loss. Therefore, no seasonal changes in canopy structural parameters were taken into account.

3.2.2.2. Wet-canopy evaporation. The average wet-canopy evaporation rate ($\bar{E}$) was estimated in three ways. A first estimate of $\bar{E}$ was obtained using the wet-canopy variant of the Penman-Monteith equation (hereafter referred to as E_{PM}), where the canopy resistance (r_s) was set to zero (Monteith, 1965) and the aerodynamic resistance (r_a, s m^{-1}) was calculated using the wind speed and forest roughness characteristics (based in turn on mean forest height) following Thom (1975). To determine the net radiant energy above the canopy from the incoming short-wave radiation as measured in the nearby degraded fire-climax grassland, albedo values of 0.150 (Oguntoyinbo, 1970; Giambelluca et al., 1997) and 0.135 (Giambelluca et al., 1997, 1999) were used for the YSF and SMF, respectively, in conjunction with the Brunt formula for the estimation of net long-wave radiation (Kijne, 1973). The net soil heat flux was assumed to be negligible (cf. Hölscher et al., 1997). The evaporation rate derived in this way represents the rate per unit area of canopy cover. A second estimate of $\bar{E}$ was obtained from the slope of the linear regression of precipitation (P) against interception loss (I), which according to Gash (1979) has a slope of $\bar{E}/\bar{R}$, in combination with the average rainfall intensity during saturated canopy conditions ($\bar{R}$) as derived from the tipping bucket recorder. The value of $\bar{E}$ derived in this way is referred to as the Tf-based average wet-canopy evaporation rate per unit ground area (E_{Tf}). A third estimate of $\bar{E}$ (also per unit ground area) was obtained through optimization of $\bar{E}/\bar{R}$ by minimizing the sum of the squared differences between the observed and modeled interception losses (least squares method, hereafter referred to as E_{OPT}) (Marquardt, 1963).

4. Results

4.1. Rainfall event characteristics

The analyses were carried out for the period 1 October 2014–30 September 2015, which encompasses a complete hydrological year in the region. During these 12 months, total rainfall was 1747 mm at the SMF and 1629 mm at the YSF site. These amounts were slightly above (SMF) or very similar (YSF) to the long-term (1983–2013) mean annual rainfall of 1625 mm measured at Andasibe (located ca. 2 km from the SMF and 3 km from the YSF) (Météo Madagascar, 2013). Rainfall at both study sites was highly seasonal: approximately 80% of the annual rainfall occurred during the wet season (November–April) (Fig. 3; cf. Table 4). Monthly rainfall showed a unimodal cycle, with the highest rainfall in February (Fig. 3).

A total of 246 discrete rainfall events were recorded at the SMF plot vs. 254 at the YSF plot. The average (median) event-based rainfall amount, duration and intensity of rainfall at the SMF plot were 6.95 (2.0) mm, 5 h (3 h 20 min), and 1.72 (0.78) mm h^{-1}, respectively (Table 3). Corresponding values for the YSF plot were 6.24 (1.89) mm, 4 h 20 min (2 h 55 min) and 2.00 (0.95) mm h^{-1}, respectively. The average (±SD) time between successive events at both sites was ~30 ± 45 h, indicating approximately one event per day. The frequency distributions of event size, rainfall intensity, and duration for the study period are shown in Fig. 4. There was no significant difference between the SMF and YSF for any of these rainfall characteristics ($p < 0.05$; Mann-Whitney U test). For approximately 70% of the rainfall events, total rainfall was less than 5 mm, while for 10% of the events, amounts were between 5 and 10 mm. Likewise, 38% of the events at both sites had a duration of less than 2 h. Approximately 80% of the events were delivered at an average intensity of less than 2.5 mm h^{-1}. Rainfall at both sites occurred most frequently between 14:00 and 24:00 h (representing ~63% of total rainfall), reflecting the prevalence of convective rainfall (Fig. 5).

To assess inter-seasonal variability in rainfall characteristics, rainfall properties were analyzed separately for the wet (November–April) and the dry (May–October) season. Events smaller than 5 mm were more common during the dry season (90% of events) than in the wet season (60%) (Fig. 6). Larger rainfall events (>20 mm) occurred most frequently during the wet season. The average rainfall intensity was also lower during the dry season when about 90% of the events had an average intensity of less than 2.5 mm h^{-1} vs. 60% in the wet season.

4.2. Throughfall, stemflow and interception losses

Table 4 gives an overview of measured throughfall (Tf), stemflow (Sf) and derived estimates of the interception loss (I) for the SMF and YSF sites for the wet and the dry season. Measured Tf totals for the entire study period were 1240 and 1235 mm for the SMF and YSF plots, respectively, representing 71.0% and 75.8% of incident rainfall, respectively. Overall standard errors (SE) of the Tf estimates for the SMF and YSF were 4.3% (i.e. 53.2 mm or 3.0% of P) and 6.8% (i.e. 83.7 mm or 5.1% of P), respectively. Tf totals for the wet and dry season in the SMF were 1014 mm (73.5% of P) and 226 mm (61.4% of P), respectively (Table 4). Corresponding values for the YSF plot were 1017 mm (76.6% of P) and 218 mm (72.2% of P).

Stemflow was (much) higher for the young forest (6.2% of P) than for the semi-mature forest (1.7% of P). The SE values of the respective overall Sf estimates were 18.2% and 17.3% for the SMF and YSF. In the SMF, wet-season Sf was 27 mm (3% of P) vs. only 3 mm (0.8% of P) during the dry season, with corresponding values for the YSF being 93 mm (7% of P) and 9 mm (3% of P).

Rainfall interception losses (I) per unit ground area derived by subtracting the measured Tf and Sf from incident rainfall for the study period were 477 mm (27.3% of P) and 292 mm (17.9% of P) for the SMF and YSF, respectively. Adding the SE's of the Tf and Sf quadratically suggested SE values of 53.5 mm (3.0% of P) and 85.5 mm (5.2% of P) for overall I for the SMF and YSF, respectively. The interception loss from the SMF was significantly higher than that from the YSF ($p < 0.05$; Mann-Whitney U test). Seasonal differences in relative interception loss (I/P) were also significant (Table 4). For the SMF, wet-season interception loss was 338 mm vs. 139 mm for the dry season, representing 24.5% and 37.8% of P, respectively. Likewise, for the YSF, wet-season I was 217 mm vs. 75 mm for the dry season, representing 16.4% and 24.8% of P, respectively. Monthly I/P varied between 19.5% (February) and 49.8% (May) for the SMF and between 14.0% (February) and 35.3% (April) for the YSF (Fig. 7).

4.3. Model results

The daily throughfall and stemflow measurements were used to model interception loss for the SMF and YSF sites. Values for the canopy parameters in the revised analytical model were obtained from the calibration data-set (subset-1; Table 5, Fig. 8).

The model was run using the respective canopy parameters with three different wet-canopy evaporation rates: (1) the wet

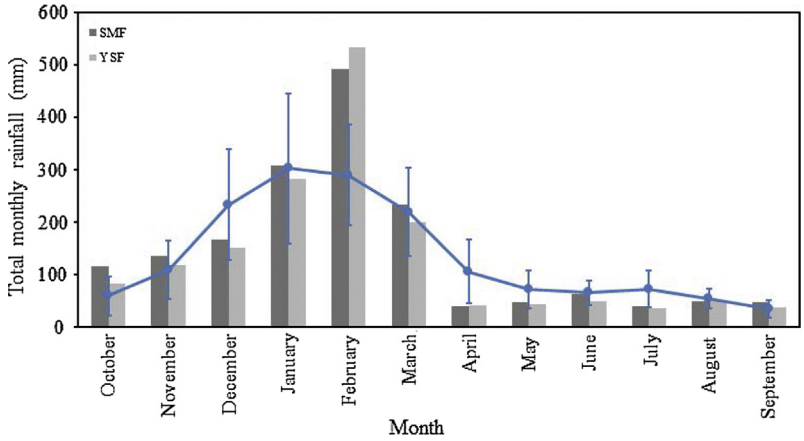

Fig. 3. Monthly rainfall at the semi-mature (SMF) and young secondary forest (YSF) plots for the one-year measurement period (1 October 2014 to 30 September 2015). The symbols indicate the mean monthly rainfall at Andasibe (1983–2013) and the error bars the standard deviation.

Table 3
Summary statistics for the rainfall events (>0.4 mm) observed during the 1 October 2014–30 September 2015 study period. SMF and YSF denote the semi-mature and young secondary forest sites, respectively.

Parameters	Rainfall (P, mm)		Duration (h: min)		Intensity (mm h^{-1})	
	SMF	YSF	SMF	YSF	SMF	YSF
Mean	6.95	6.24	5:00	4:20	1.72	2
Range	0.4–70.2	0.4–69	00:05–30:55	00:05–32:40	0.14–17.5	0.13–23.8
Median	2.00	1.89	3:20	2:55	0.78	0.92

Table 4
Wet- and dry-season total rainfall (P), throughfall (Tf), stemflow (Sf) and derived estimates of rainfall interception loss (I) in mm and as a percentage of incident rainfall for the 1 October 2014–30 September 2015 study period. SMF and YSF denote the semi-mature and young secondary forest sites, respectively. Values with a star are significantly different from each other ($p < 0.05$; Mann-Whitney U test).

Experimental plot		Wet season (November to April)				Dry season (May to October)			
		P	Tf	Sf	I	P	Tf	Sf	I
SMF	mm	1379	1014	27	338*	368	226	3	139*
	% of P		73.5	1.9	24.5		61.4	0.8	37.8
YSF	mm	1327	1017	93	217*	302	218	9	75*
	% of P		76.6	7.0	16.4		72.2	3.0	24.8

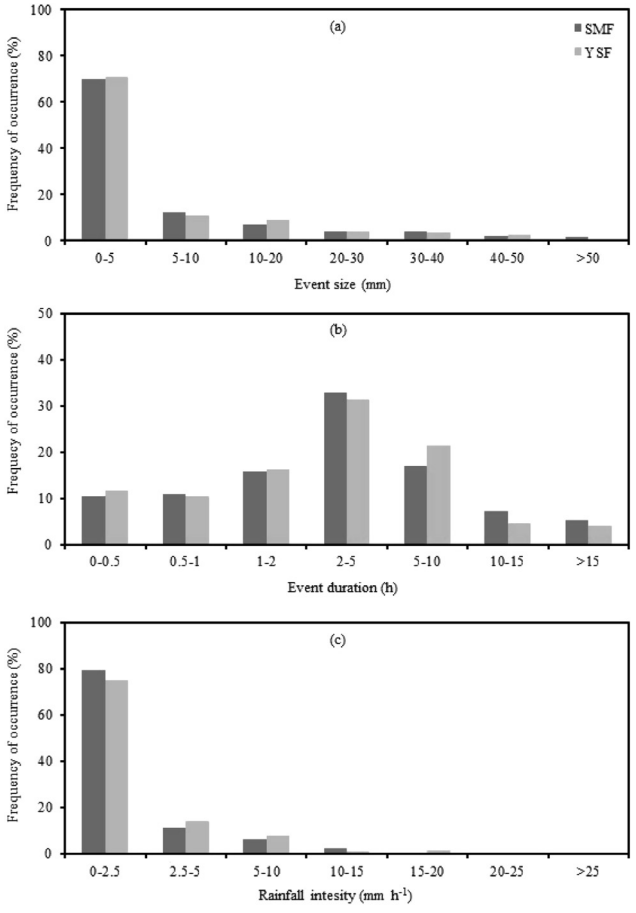

Fig. 4. Frequency distributions of: (a) amount, (b) duration, and (c) intensity of rainfall events at the semi-mature (SMF) and young secondary forest (YSF) plots during the one-year measurement period from 1 October 2014 to 30 September 2015.

variant of the Penman-Monteith equation (E_{PM}), (2) the linear regression approach (Gash, 1979) (E_{Tf}), and (3) optimizing the ratio of $\overline{E}/\overline{R}$ by least squares method (E_{OPT}). The model efficiency of each run was evaluated using the method described by Nash and Sutcliffe (1970).

Measured and predicted total interception losses for the calibration data-set (subset-1) are summarized in Table 6 and presented in Fig. 9. The first run (Model 1) used E_{PM}-values of 0.07 and 0.05 mm h^{-1} for the SMF and YSF, respectively. The median rainfall intensity falling onto a saturated canopy for this model was 1.6 mm h^{-1} for both sites. As shown in Fig. 9, predicted interception losses were 49% (SMF) to 60% (YSF) lower than observed losses and the model efficiency was very low (<0.2; Table 6). A much better fit between observed and modeled interception losses was obtained using $\overline{E}/\overline{R}$ values of 0.17 and 0.13, as derived from the regressions of I vs. P for the SMF and YSF, respectively (Model 2 using E_{Tf}). The efficiency obtained for Model 2 was > 0.8 but the model overestimated I in the SMF by 2.3% and that in the YSF by 9.4%. The performance of Model 3 (using E_{OPT}) was slightly better than that of Model 2 for the YSF in terms of cumulative modeled I (Table 6). For the SMF, optimization (Model 3) did not have an effect on cumulative modeled I nor on model efficiency (Table 6). Model 3 yielded E_{OPT}-values of 0.27 mm h^{-1} and 0.20 mm h^{-1} for the SMF and YSF, respectively. Using the latter, predicted interception losses agreed very well with the observed values for both forests for the validation data-set (Table 6; Fig. 10). Because Tf-based wet-canopy evaporation rates are obtained from observations in a more direct manner (see Section 3.2.2.2), the performance of the model was also tested using E_{Tf} and the estimated canopy parameters from the calibration data-set. The predicted total interception losses for the validation data-set using E_{Tf} were also in very good agreement with those derived from the Tf and Sf measurements, with relative errors of < 7% and model efficiencies above 0.85 for both sites (Table 6; Fig. 10).

Analysis of the contributions to overall modelled I by the five different interception components distinguished in the model (cf. Table 2) revealed that most of the total interception loss occurred during saturated canopy conditions (i.e., during phase 2); 50% in the SMF and 62% in the YSF (Table 7). The next largest term was evaporation from the canopy after rainfall had ceased (i.e. the drying-up phase), with the SMF having a bigger loss of this kind (34%) than the YSF (25%). Small rainfall events also contributed significantly to overall interception losses (11% in the SMF vs. 9% in the YSF), whereas losses associated with evaporation from trunks were minor (<1.5%).

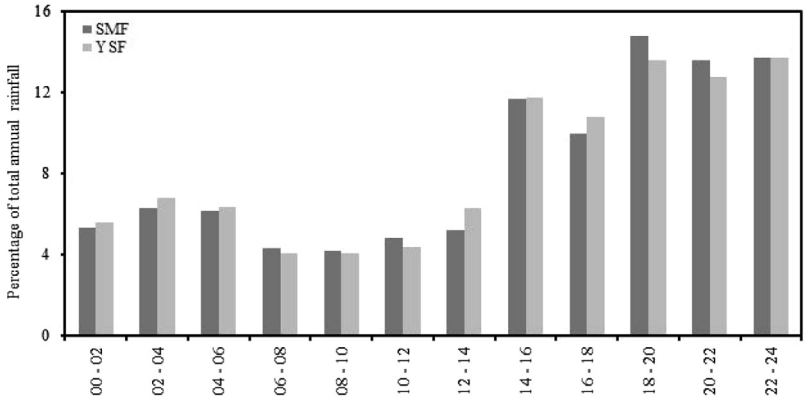

Fig. 5. Diurnal distribution of rainfall amounts for the one-year measurement period (1 October 2014 to 30 September 2015) at the semi-mature (SMF) and young secondary (YSF) forest plots.

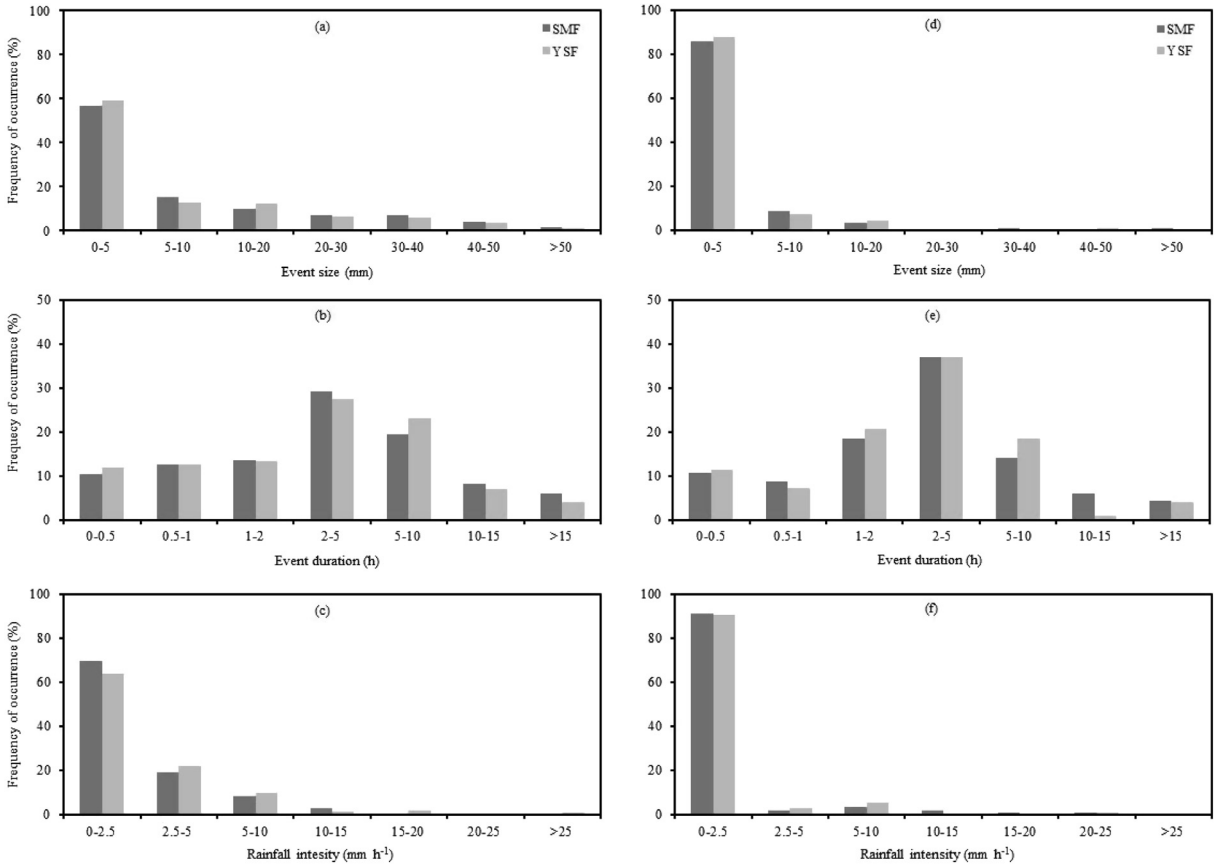

Fig. 6. Frequency distributions of: (a) amount, (b) duration, and (c) intensity of rainfall events during the wet (left-hand panels: a, b, c) and dry (right-hand panels: d, e, f) season. SMF denotes the semi-mature and YSF the young secondary forest.

5. Discussion

5.1. Rainfall

The observed difference of 118 mm in total rainfall between the two study sites is not unexpected considering that they are located ca. 2 km apart in complex terrain with possible local rain shadows (on more leeward slopes like the YSF site) and precipitation 'hot spots' (on more windward slopes like the SMF site). However, at 6.7% the difference in total precipitation is relatively small. Moreover, a double mass analysis of daily rainfall totals for our two sites (see Supplementary material) did not reveal any systematic bias towards one station or the other, suggesting the spatial variation in rainfall to be random and not the result of differences in site exposure. Regionally, rainfall in Madagascar is primarily associated with warm and moist air masses originating over the Indian Ocean that rain-out as they rise and pass the steep mountains in the East, leaving less moisture for rainfall generation in the sheltered western part of the island (Tadross et al., 2008). Among the few quantitative studies of rainfall patterns in Madagascar, Griffiths and Ranaivoson (1972) identified geographical location, distance to the ocean, and wind regime as the prime factors governing climatic conditions across the island.

The seasonal variation in rainfall is strongly influenced by the Indian monsoon, trade-wind circulations and occurrence of tropical cyclone events (Riehl, 1979; Hastenrath, 1985; Jury et al.,

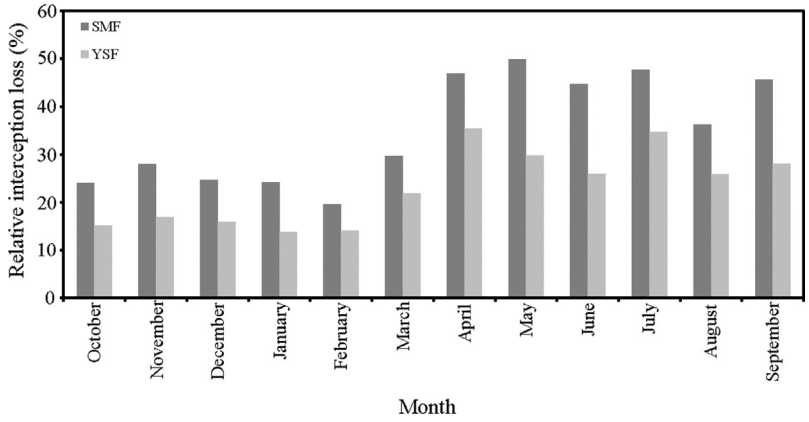

Fig. 7. Seasonal variation in the relative interception loss (I/P) for the semi-mature (SMF) and young secondary forest (YSF) for the one-year measurement period (1 October 2014 to 30 September 2015).

Table 5
Summary of canopy and climatic parameters used in the revised analytical model. SMF and YSF denote the semi-mature and young secondary forest site, respectively.

Experimental plot	Canopy-related parameters[a]					Climate-related parameters[b]				
	S (mm)	p	c	S_t (mm)	p_t	$\overline{R}$ (mm h^{-1})	E_{PM} (mm h^{-1})	E_{Tf} (mm h^{-1})	E_{OPT} (mm h^{-1})	P'_g (mm)
SMF	1.20	0.30	0.70	0.095	0.032	1.6	0.07	0.27	0.27	1.96
YSF	0.47	0.45	0.55	0.130	0.092	1.6	0.05	0.21	0.20	0.97

[a] Canopy parameters: S = canopy storage capacity; p = free throughfall coefficient; S_t = trunk storage capacity; p_t = the proportion of rain diverted to stemflow.
[b] Climatic parameters; $\overline{R}$ = median rainfall intensity falling onto a saturated canopy; E_{PM} = wet-canopy evaporation rate derived using the Penman-Monteith equation; E_{Tf} = throughfall-based estimate of wet-canopy evaporation rate; E_{OPT} = optimized wet-canopy evaporation rate; P'_g = the rainfall necessary to saturate the canopy.

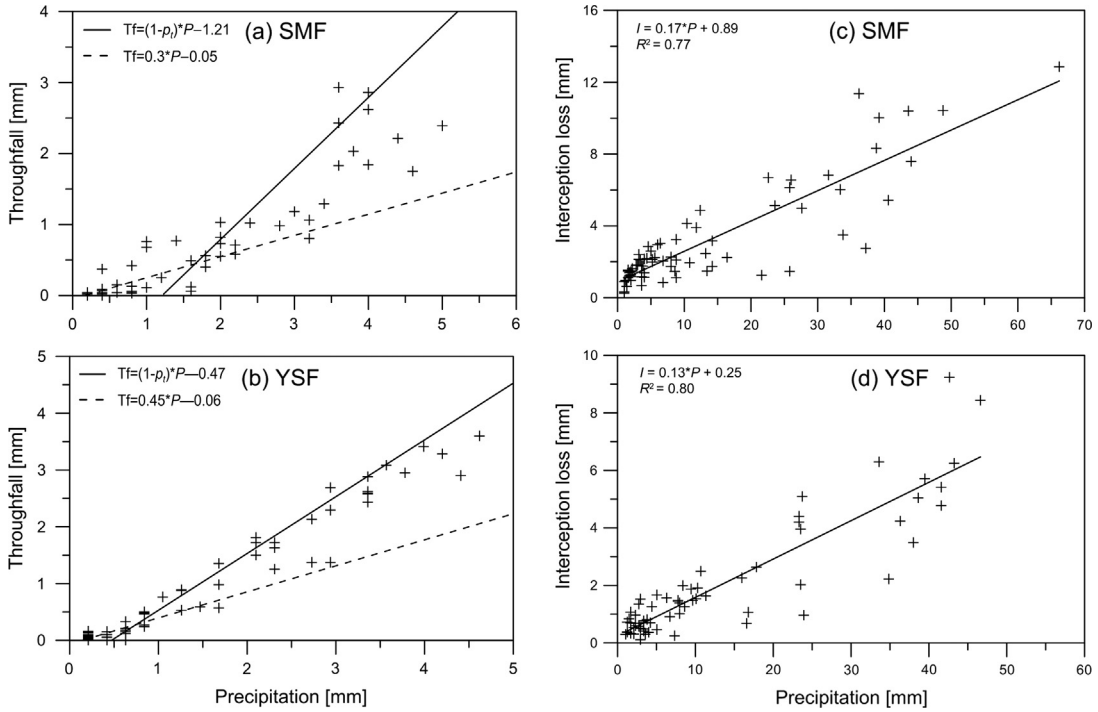

Fig. 8. Determination of the various interception model parameters for the SMF and YSF sites. (a, b) Canopy capacity S and free throughfall coefficient p according to the method of Jackson (1975); (c, d) the relative wet-canopy evaporation rate according to Gash (1979).

1995). During the wet season, rainfall is primarily associated with convective and orographic uplift of the moist oceanic air masses brought in by the easterly trade-winds, whereas during the dry season rainfall occurs mainly from stratus clouds associated with the passage of cold fronts (Tadross et al., 2008). As a result, rainfall patterns show a marked seasonal variation, with the wet season (November to April) receiving around ~80% of the annual rainfall (Fig. 3). During the study year, the wet season was generally characterized by high monthly rainfall totals and relatively high rainfall intensities (Fig. 6). In the dry season (May to October) monthly

Table 6
Comparison of observed and modelled interception losses (mm) for the semi-mature (SMF) and young (YSF) secondary forest sites.

	Calibration data (set 1*)						Validation data (set 2*)			
	Model 1 (E_{PM})		Model 2 (E_{Tf})		Model 3 (E_{OPT})		Model 2 (E_{Tf})		Model 3 (E_{OPT})	
	SMF	YSF	SMF	YSF	SMF	YSF	SMF	YSF	SMF	YSF
Total gross rainfall (mm)	1048	1027	1048	1027	1048	1027	699	602	699	602
Total modeled interception loss (mm)	133	64	267	174	267	170	211	126	211	123
Total measured interception loss (mm)	261	159	261	159	261	159	217	132	217	132
Relative error (%)	−49	−59.7	2.3	9.4	2.3	6.9	2.7	−6.15	2.7	−6.7
Nash-Sutcliffe model efficiency	0.19	0.05	0.83	0.82	0.83	0.83	0.87	0.89	0.87	0.89

set 1* = November, January, Feb, May, June.
set 2* = October, December, March, April, May, July, September.

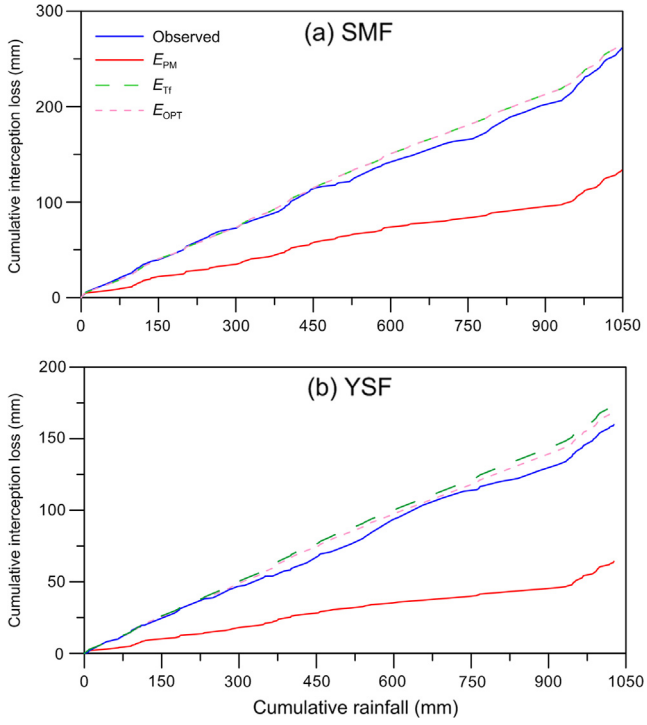

Fig. 9. Cumulative measured and modeled interception losses for (a) the semi-mature secondary forest (SMF) and (b) the young secondary forest (YSF) site for the calibration data-set. Modelled interception losses were calculated for each site using wet-canopy evaporation rates estimated with the Penman-Monteith equation (E_{PM}); a throughfall-based wet-canopy evaporation rate (E_{Tf}), and an optimized value (E_{OPT}). See Table 6 for goodness of fit indicators for the respective models.

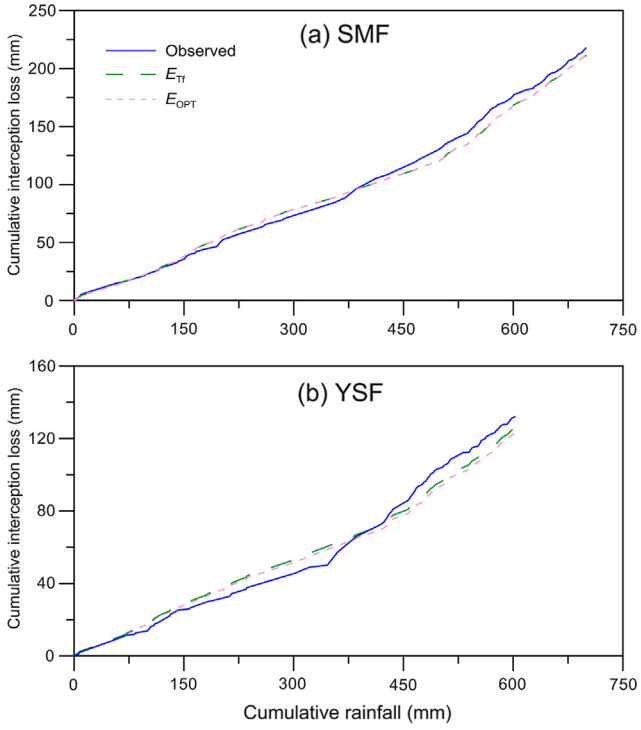

Fig. 10. Cumulative measured and modelled interception losses for (a) the semi-mature secondary forest (SMF) and (b) the young secondary forest (YSF) site for the validation data-set using a throughfall-based wet-canopy evaporation rate (E_{Tf}) and an optimized value (E_{OPT}). See Table 6 for goodness of fit indicators for the respective models.

rainfall totals were very low and most of the rain fell during low-intensity events (<2.5 mm h^{-1}). Comparative information based on the analysis of 5-min rainfall records for similar elevations elsewhere in the tropics is limited. In addition, rainfall intensity distributions are often heavily skewed (cf. Fig. 4c), rendering comparisons of average rather than median values somewhat problematic (cf. Schellekens et al., 1999; Wallace and McJannet, 2008). Nevertheless, the average wet-season rainfall intensity of 2.5 mm h^{-1} at the two study sites (at elevations of 950–990 m.a.s.l) is lower than the 3–5 mm h^{-1} range typically reported for other tropical lower montane sites (350–1100 m.a.s.l.) (e.g. Schellekens et al., 1999; van Dijk and Bruijnzeel, 2001b; Wallace and McJannet, 2008, 2012), while the average intensity for the dry season (1.8 mm h^{-1}) resembles values found for comparable lower montane tropical climates more closely (1–3 mm h^{-1}; e.g. Fleischbein et al., 2005; Wallace and McJannet, 2008, 2012).

Table 7
Components of the interception loss in mm (and as a percentage of the total) for the 1 October 2014 – 30 October 2015 study period, based on the calibrated revised analytical model (Gash et al., 1995) with the optimized wet canopy evaporation rate (E_{OPT}). SMF and YSF denote the semi-mature and young secondary forest sites, respectively.

Interception component (mm)	SMF	SMF
m small storms ($< P'_g$) insufficient to saturate canopy	50.9 (10.7%)	25.8 (8.7%)
Wetting up of the canopy; n storms $> P'_g$ which saturate canopy	24.3 (5.1%)	10.8 (3.7%)
Evaporation from saturated canopy	236.8 (49.5%)	182.5 (61.7%)
Evaporation from canopy after storms	162 (33.4%)	72.8 (24.7%)
Evaporation from stems	4.3 (0.9%)	3.8 (1.3%)
Total modelled interception loss	478	296
Total measured interception loss	476	292

5.2. Stemflow, throughfall and rainfall interception loss

Our observations showed that stemflow Sf was distinctly higher for the YSF (102 mm, 6.2% of *P*) than for the SMF (30 mm, 1.7%). The reason for this large difference may well be the crown morphology of the dominant tree (*Psiadia altissima*) in the young forest, which had strongly upward-thrusting branches. Steep branches have a greater potential for contributing to Sf than do more horizontal or drooping branches, which were more prevalent in the SMF (cf. Herwitz, 1987; Murakami, 2009). Although the dependence of stemflow amounts on forest age involves a number of complex processes in which bark storage capacity (S_t) is thought to play a significant role (Levia and Herwitz, 2005), the S_t-values derived for the SMF (0.095 mm) and YSF (0.130 mm) hardly differed and appear to be too small to have a major effect on Sf. Stemflow can be a significant fraction of precipitation (23–41% of *P*) in some young secondary forests dominated by palm- and banana-like pioneer species in Amazonia (Hölscher et al., 1998; Schrott et al., 1999) but elsewhere, reported Sf values were small (1–1.5%; Macinnis-Ng et al., 2014) or even neglected (Zimmermann et al., 2013). Intermediate values (5–7% of *P*) have been reported for a semi-deciduous secondary forest of intermediate age in upland Mexico (ca. 20 years old; Holwerda et al., 2010), while under temperate conditions Sf tends to be higher during the leafless season as well (Levia and Germer, 2015). As such, comparative information on the importance of stemflow in different types of tropical secondary forests is scant and our understanding of the chief controlling factors is still very limited.

Our results provide the first quantitative information on rainfall interception losses by secondary tropical forests in Madagascar. Although comparative data for similarly aged secondary forests elsewhere in the tropics are scarce, the observed interception loss for the semi-mature forest (27.3% of *P*) is comparable to that reported for old-growth lower montane rain forests (28 ± 7% of *P*; Bruijnzeel et al., 2011). Likewise, Zimmermann et al. (2013) noted that interception losses for regrowth older than 10 years in lowland Panamá were not statistically distinguishable from those for nearby old-growth rain forest. This finding was confirmed for a lower montane situation in Panamá by Macinnis-Ng et al. (2014). However, major increases in *I*/*P* were inferred by Zimmermann et al. (2013) during the first 10 years of forest regrowth. Comparing the interception loss for the 5–7-year-old YSF (18% of *P*) with similarly aged young secondary forest in (lowland) Central Panamá (7–12%, ignoring negative interception values for two out of seven stands; Zimmermann et al., 2013) shows that the interception losses are much larger for the Malagasy forest. This difference is likely to be caused by the low rainfall intensities (75% arriving at <2.5 mm h^{-1}) and frequent occurrence of small rainfall events (~70% <5 mm each) in the study area compared to rainfall in Central Panamá, where most events are short and intense (Ogden et al., 2013). Indeed, our modeling exercise indicated that a large proportion of overall interception loss in the YSF occurred during saturated canopy conditions (Table 5). However, the range of the average (short-term, 2 months) Tf values obtained by Zimmermann et al. (2013) for seven 5–7-year-old forests was considerable (87.3–101.6% of *P*). Because negative interception values were inferred for two stands, despite the fact that stemflow was considered to be negligible, it cannot be excluded that the 20 (fixed) Tf collectors used by Zimmermann et al. (2013) may not have been sufficient to adequately capture the spatial variability of Tf in some stands and that this measurement uncertainty also contributes to the differences between the two areas. However, the use of a larger number of gauges usually leads to higher, rather than lower, mean Tf totals because of the inclusion of a more representative number of 'drip points', where Tf is typically concentrated (Lloyd and de Marques-Filho, 1988; Holwerda et al., 2006). More work is, thus, needed in differently structured secondary tropical forests. Indeed, the dynamic interplay between storm frequency, duration and intensity vis á vis canopy storage capacity constitutes an important and dominant aspect of the interception process in tropical forests, be it old-growth forest (Lloyd, 1990; Zeng et al., 2000; Cuartas et al., 2007; Wallace and McJannet, 2008), plantation forest (Bruijnzeel and Wiersum, 1987; Hall, 2003) or regenerating forest (Zimmermann et al., 2013; Macinnis et al., 2014; cf. Table 4).

Considering that interception losses are usually higher for denser and taller tropical forests having a higher LAI (Fleischbein et al., 2005; Dietz et al., 2006; Wallace and McJannet, 2008; Wallace et al., 2013; Zimmermann et al., 2013), while overall weather conditions experienced by our two stands were quite similar due to their proximity and comparable elevation, the higher interception loss derived for the SMF can be explained largely by the difference in forest structure (notably greater tree density, height and LAI). Therefore, it is expected that the observed difference in interception loss between the SMF and YSF will become smaller and eventually disappear as forest height and LAI at the YSF increase. The rapid increase in interception loss and soil water uptake during the early years of tropical forest succession when leaf area increases rapidly (Hölscher et al., 2005; Giambelluca, 2002) may well impact the catchment water balance negatively (Swank et al., 2001; Beck et al., 2013; Lacombe et al., 2015), even more so if these changes in vegetation water use predate the recovery of top-soil infiltration capacity and associated soil water replenishment (Ziegler et al., 2004; Zimmermann et al., 2013).

5.3. Wet-canopy evaporation

Wet-canopy evaporation rates derived using the Penman-Monteith equation for the SMF (0.07 mm h^{-1}) and YSF (0.05 mm h^{-1}) fall in the lower range of estimates of E_{PM} for other lower montane tropical forests (0.06–0.16 mm h^{-1}; Schellekens et al., 1999; Wallace and McJannet, 2008; Holwerda et al., 2012). Correcting E_{Tf} for canopy cover fraction to allow direct comparisons to be made with E_{PM}-values gave average E_c-values of ~0.38 mm h^{-1} for both the SMF and YSF, which is about five (SMF) to seven (YSF) times higher than the corresponding E_{PM}-values. The optimized wet-canopy evaporation rates were very close to the E_{Tf} values (Table 5). Nevertheless, the Tf-based wet-canopy evaporation rates (0.27 mm h^{-1} per unit ground surface area for the SMF and 0.21 mm h^{-1} for the YSF) are much lower than values reported for several other tropical lower montane rain forests situated in similar topography as our study sites (0.46–1.2 mm h^{-1}; Schellekens et al., 1999; Wallace and McJannet, 2008; Holwerda et al., 2012). Such discrepancies are likely to be caused in part by differences in canopy roughness and density. The YSF and SMF had LAI values of 1.8 and 3.4 m^2 m^{-2} (Table 1) and 55–70% canopy cover (Table 5) compared to 4.1–5.9 m^2 m^{-2} (77–97% canopy cover) for the old-growth lower montane forests studied by Wallace and McJannet (2008), Schellekens et al. (1999) and Holwerda et al. (2012). While our E_c-values (~0.38 mm h^{-1}) are comparable to the 0.47 mm h^{-1} derived for the Mt. Lewis site in northern Queensland, E_c-values for similar forest at Upper Barron (Queensland, 0.84 mm h^{-1}; Wallace and McJannet, 2008) and in Puerto Rico (0.82 mm h^{-1}; Holwerda et al., 2012) remained much higher, suggesting local physiographic factors affecting site evaporation climate (e.g., aspect, elevation and distance to the ocean) to be more important than canopy structural characteristics (see discussion in Holwerda et al., 2012). Yet, the observed similarity in wet-canopy evaporation rates (E_c) for the two studied forests with their very different structural characteristics (Table 1) may hint at the possibility to generalize E_c for different forest types in the study area (cf. Miralles et al., 2010).

5.4. Performance of the revised analytical model

The revised version of the analytical model of rainfall interception predicted the interception values for the SMF and YSF sites satisfactorily (Table 6) and also captured intra-annual variations well. The difference between observed and simulated I is (much) smaller than reported for a number of other tropical interception modeling studies (e.g. Calder et al., 1986; Bruijnzeel and Wiersum, 1987; Lloyd et al., 1988; Schellekens et al., 1999; Wallace and McJannet, 2008; Fan et al., 2014). Optimizing $\overline{E}/\overline{R}$ during model calibration had little (YSF) to no (SMF) effect on overall model performance compared to the results obtained using Tf-based wet-canopy evaporation rates (Table 6).

One of the main assumptions of the analytical model is that the average intensity of rain falling on a saturated canopy ($\overline{R}$), canopy storage capacity (S), and wet-canopy evaporation rate ($\overline{E}$) are constant in time. It is likely that $\overline{E}$ will vary seasonally with weather conditions, while S may vary in response to changes in LAI (Van Dijk and Bruijnzeel, 2001a,b; Fleischbein et al., 2005). Moreover, $\overline{R}$ at the study sites increased from 1.8 mm h^{-1} in the dry season to 2.5 mm h^{-1} in the wet season (cf. Fig. 6). Although the effect of seasonal variation in rainfall intensity was minimized by using both wet- and dry-season data during model calibration, it was considered to be of interest to also explore the possible consequences of intra-annual variation in rainfall and weather on model performance. The revised analytical interception model was therefore re-run separately for each site for the dry (May–October) and wet season (November–April). In doing so, the focus was primarily on evaluating changes in the relative evaporation rate ($\overline{E}/\overline{R}$) for the respective seasons because previous studies suggested that the analytical model is highly sensitive to variations in climatic parameters and less sensitive to changes in the canopy parameters S and c (Dykes, 1997; Fan et al., 2014; Pereira et al., 2016). Somewhat surprisingly in view of the contrast in mean rainfall intensities between the two seasons, separating the two seasons gave effectively the same overall relative evaporation rates ($\overline{E}/\overline{R}$ = 0.17 for the SMF and 0.13 for the YSF) as obtained using the regression method for the calibration data-set. Because values of E_{Tf} were also lower during the dry season (0.22 and 0.16 mm h^{-1} for the SMF and YSF, respectively), overall model performance remained the same. The fact that relative interception losses were 8% (YSF) to 13% (SMF) higher in the dry season compared to the wet season (Table 4) reflects the more frequent occurrence of small storms and to a lesser extent the lower rainfall intensity observed during the dry season (cf. Fig. 6). This also means that seasonal variations in I/P are affected mostly by the number of small rainfall events. A similar conclusion was reached by Wallace and McJannet (2008) for a series of rain forests at different elevations in northern Queensland on the basis of a small improvement in the analytical model's performance when running the model separately for the wet and dry season. The present model results also suggest that a generally good parameterization of the revised analytical model can be achieved by inclusion of rainfall and interception data from both wet and dry seasons during model calibration, which can be used subsequently to estimate interception losses at any time of the year.

6. Conclusion

Rainfall interception losses were quantified and modeled for a semi-mature (ca. 20-years-old) and a young (5–7 years) secondary forest in Eastern Madagascar. Over the one-year study period, measured throughfall, stemflow and derived estimates of interception loss for the semi-mature forest (SMF) were 71.0%, 1.7% and 27.3% of incident rainfall, respectively. Corresponding values for the young secondary forest (YSF) were 75.8%, 6.2% and 18.0%. Given the similarity in climatic conditions experienced by the two stands, the observed difference in interception loss between the two forests can be explained largely by their contrasting structure (notably higher tree density, height and leaf area index in the SMF). The high fraction of stemflow for the YSF is thought to reflect the strongly upward-thrusting habit of the branches of the dominant species (*Psiadia altissima*), which favours funneling of precipitation. The revised analytical interception model (Gash et al., 1995) was used for the first time to simulate interception evaporation from tropical secondary forest. The model was able to reproduce cumulative interception losses at the two sites accurately and succeeded in capturing the seasonal variability in interception loss associated with the variability in the rainfall characteristics, provided that a throughfall-based value for the average wet-canopy evaporation rate was used (instead of values based on the Penman-Monteith equation). Analysis of the magnitude of the different interception components distinguished by the model revealed that most of the overall interception loss occurred during saturated canopy conditions and after evaporation from the canopy after rainfall had ceased. Small rainfall events also contributed significantly to the total interception loss. The model further indicated that seasonal variations in either wet-canopy evaporation rate ($\overline{E}$) or average rainfall intensity ($\overline{R}$) (both lower during the dry season) had little or no effect on model performance because the relative evaporation rate ($\overline{E}/\overline{R}$) did not change significantly throughout the year. Our results thus confirm earlier findings that increases in canopy interception during tropical forest regrowth can be rapid and that some regenerating stands re-evaporate an important part of the rainfall. This may affect the water balance during forest succession, depending on the balance between corresponding changes in soil water uptake (transpiration) and replenishment (through improved infiltration).

Acknowledgements

Funding for this research was provided by the Ecosystem Services for Poverty Alleviation (ESPA) programme of the United Kingdom as part of the P4GES (Can Paying 4 Global Ecosystem Services values reduce poverty?) project (NE/K010220/1). We acknowledge the indispensable help in the field received from Andrianavonona Jean Yves, Jaona Lahitiana, Ramarolahy Georges, Randriatahina Jean Claude, Razafimanantsoa Jean Marcel, Tsiresy Rolland, Razafimahepa Réné Frederic, Youssouf and Mad Randrianasolo. We would further like to thank Mitisinjo staff for their hospitality and for allowing access to the sites. We are grateful to the Laboratoire des Isotopes (University of Antananarivo) for logistical support and Julia Jones (Bangor University) for her support and encouragement. We also thank Murat Ucer from ITC-UT for the supply and construction of equipment and Frans Backer (VU University Amsterdam) for the use of the throughfall gutters. The manuscript benefitted from the constructive comments from the editor, the associate editor and two anonymous reviewers, whose efforts are gratefully acknowledged.

Appendix A. Supplementary material

Supplementary data associated with this article can be found, in the online version, at http://dx.doi.org/10.1016/j.jhydrol.2016.10.032.

References

Aide, T.M., Grau, H.R., 2004. Globalization, migration, and Latin American ecosystems. Science 305 (5692), 1915–1916.

Bailly, C., de Coignac, G.B., Malvos, C., Ningre, J.M., Sarrailh, 1974. Étude de l'influence de couvert naturel et de ses modifications á Madagascar: experimentations en bassins versants élémentaires. Centre Technique Forestier Tropical, Nogent-sur-Marne, Cahiers Scientifiques, No. 4, 114 pp.

Beck, H.E., Bruijnzeel, L.A., van Dijk, A.I.J.M., McVicar, T.R., Scatena, F.N., Schellekens, J., 2013. The impact of forest regeneration on streamflow in 12 mesoscale humid tropical catchments. Hydrol. Earth Syst. Sci. 17, 2613–2635.

Bruijnzeel, L.A., 2004. Hydrological functions of tropical forests: not seeing the soil for the trees? Agric. Ecosyst. Environ. 104 (1), 185–228.

Bruijnzeel, L.A., Wiersum, K.F., 1987. Rainfall interception by a young *Acacia auriculiformis* (A. Cunn.) plantation forest in West Java, Indonesia: application of Gash's analytical model. Hydrol. Process. 1 (4), 185–228.

Bruijnzeel, L.A., Mulligan, M., Scatena, N.F., 2011. Hydrometeorology of tropical montane cloud forests: emerging patterns. Hydrol. Process. 25 (3), 465–498.

Calder, I.R., Wright, I.R., Murdiyarso, D., 1986. A study of evaporation from tropical rainforest, West Java. J. Hydrol. 89 (1–2), 13–31.

Carlson, K.M., Curran, L.M., Asner, G.P., Pittman, A.M., Trigg, S.N., Adeney, J.M., 2013. Carbon emissions from forest conversion by Kalimantan oil palm plantations. Nat. Clim. Change 3, 283–287.

Chazdon, R., 2014. Second Growth: The Promise of Tropical Forest Regeneration in an Age of Deforestation. University of Chicago Press, Chicago, USA.

Conservation International, 2011. Ankeniheny-Zahamena Corridor, a field demonstration model. In: Satoyama Initiative, Antananarivo, 10 pp. [Online] URL: <http://satoyama-initiative.org/en/ankeniheny-zahamena-corridor-a-field-demonstration-model-conservation-international-madagascar/>.

Crk, T., Uriarte, M., Corsi, F., Flynn, D., 2009. Forest recovery in a tropical landscape: what is the relative importance of biophysical, socioeconomic, and landscape variables? Landscape Ecol. 24, 629–642.

Cuartas, L.A., Tomasella, J., Nobre, A.D., Hodnett, M.G., Waterloo, M.J., Múnera, J.C., 2007. Interception water-partitioning dynamics for a pristine rainforest in Central Amazonia: marked differences between normal and dry years. Agric. For. Meteorol. 145 (1–2), 69–83.

Dietz, J., Hölscher, D., Leuschner, C., Hendrayanto, 2006. Rainfall paritioning in relation to forest structure in differently managed montane forest stands in Central Sulawesi, Indonesia. For. Ecol. Manage. 237 (1–3), 170–178.

Du Puy, D., Moat, J., 1996. A refined classification of the primary vegetation of Madagascar based on the underlying geology: using GIS to map its distribution and to assess its conservation status. In: Lourenço, W.R. (Ed.), International symposium on the 'Biogéographie de Madagascar'. Editions de l'ORSTOM, France, Paris, pp. 205–218.

Dykes, A.P., 1997. Rainfall interception from a lowland tropical rainforest in Brunei. J. Hydrol. 200 (1–4), 260–279.

Fan, J., Oestergaard, K.T., Guyot, A., Lockington, D.A., 2014. Measuring and modelling rainfall interception losses by a native *Banksia* woodland and an exotic pine plantation in subtropical coastal Australia. J. Hydrol. 515, 156–165.

FAO (Food and Agriculture Organization of the United Nations), 2010. Global Forest Resources Assessment 2010. FAO Forestry Paper, No. 163. FAO, Rome, Italy.

Fleischbein, K., Wilcke, W., Goller, R., Boy, J., Valarezo, C., Zech, W., Knoblich, K., 2005. Rainfall interception in a lower montane forest in Ecuador: effects of canopy properties. Hydrol. Process. 19 (7), 1355–1371.

Fox, J., Truong, D.M., Rambo, A.T., Tuyen, N.P., Cuc, L.T., Leisz, S., 2000. Shifting cultivation: a new old paradigm for managing tropical forests. Bioscience 50 (6), 521–528.

Fox, J., Fujita, Y., Ngidang, D., Peluso, N.L., Potter, L., Sakuntaladewi, N., Sturgeon, J., Thomas, D., 2009. Policies, political economy, and swidden, in Southeast Asia. Hum. Ecol. 37 (3), 305–322.

Gash, J.H.C., 1979. An analytical model of rainfall interception by forests. Quart. J. Roy. Meteorol. Soc. 105 (443), 43–55.

Gash, J.H.C., Morton, A.J., 1978. An application of the Rutter model to the estimation of the interception loss from Thetford Forest. J. Hydrol. 38 (1–2), 49–58.

Gash, J.H.C., Lloyd, C.R., Lachaud, G., 1995. Estimating sparse forest rainfall interception with an analytical model. J. Hydrol. 170 (1–4), 79–86.

Geist, H.J., Lambin, E.F., 2002. Proximate causes and underlying driving forces of tropical deforestation. Bioscience 52 (2), 143–150.

Giambelluca, T.W., 2002. Hydrology of altered tropical forest. Hydrol. Process. 16 (8), 1665–1669.

Giambelluca, T.W., Nullet, M.A., Ziegler, A.D., Tran, L., 2000. Latent and sensible heat energy flux over deforested land surfaces in the eastern Amazon and northern Thailand. Singap. J. Trop. Geogr. 21 (2), 107–130.

Giambelluca, T.W., Fox, J., Yarnasarn, S., Onibutr, P., Nullet, M.A., 1999. Dry-season radiation balance of land covers replacing forest in northern Thailand. Agric. For. Meteorol. 95 (1), 53–65.

Giambelluca, T.W., Hölscher, D., Bastos, T.X., Frazão, R.R., Nullet, M.A., Ziegler, A.D., 1997. Observations of albedo and radiation balance over post-forest land surfaces in the eastern Amazon basin. J. Clim. 10, 919–928.

Griffiths, J.F., Ranaivoson, R., 1972. Madagascar. In: Climates of Africa. World Survey of Climatology, vol. 10. Elsevier, Amsterdam, pp. 313–348.

Grubb, P.J., 1977. Control of forest growth and distribution on wet tropical mountains: with special reference to mineral nutrition. Annu. Rev. Ecol. Syst. 8, 83–107.

Hassler, S., Zimmermann, B., van Breugel, M., Hall, J., Elsenbeer, H., 2011. Recovery of saturated hydraulic conductivity under secondary succession on former pasture in the humid tropics. For. Ecol. Manage. 261, 1634–1642.

Hall, R.L., 2003. Interception as a function of rainfall and forest types: stochastic modelling for tropical canopies revisited. J. Hydrol. 280 (1–4), 1–12.

Herwitz, S.R., 1987. Raindrop impact and water flow on the vegetative surfaces of trees and the effects on stemflow and throughfall generation. Earth Surf. Proc. Land. 12 (4), 425–432.

Holwerda, F., Scatena, F.N., Bruijnzeel, L.A., 2006. Throughfall in Puerto Rican lower montane rain forest: a comparison of sampling strategies. J. Hydrol. 327 (3), 592–602.

Holwerda, F., Bruijnzeel, L.A., Muñoz-Villers, L.E., Equihua, M., Asbjornsen, H., 2010. Rainfall and cloud water interception in mature and secondary lower montane cloud forests of central Veracruz, Mexico. J. Hydrol. 384 (1–2), 84–96.

Holwerda, F., Bruijnzeel, L.A., Scatena, F.N., Vugts, H.F., Meesters, A.G.C.A., 2012. Wet canopy evaporation from a Puerto Rican lower montane rain forest: the importance of realistically estimated aerodynamic conductance. J. Hydrol. 414–415, 1–15.

Hölscher, D., Mackensen, J., Roberts, J.M., 2005. Forest recovery in the humid tropics: changes in vegetation structure, nutrient pools and the hydrological cycle. In: Bonell, M., Bruijnzeel, L.A. (Eds.), Forests, Water and People in the Humid Tropics. Cambridge University Press, Cambridge, UK, pp. 598–621.

Hölscher, D., Köhler, L., Keuschner, Chr., Kappelle, M., 2003. Nutrient fluxes in stemflow and throughfall in three successional stages of an upper montane rain forest in Costa Rica. J. Trop. Ecol. 19 (5), 557–565.

Hölscher, D., de Sá, T.D.A., Bastos, T.X., Denich, M., Fölster, H., 1997. Evaporation from young secondary vegetation in eastern Amazonia. J. Hydrol. 193 (1–4), 293–305.

Hölscher, D., de Sá, T.D.A., Möller, R.F., Denich, M., Fölster, H., 1998. Rainfall partitioning and related hydrochemical fluxes in a diverse and in a mono-specific (*Phenakospermum guyannense*) secondary vegetation stand in eastern Amazonia. Oecologia 114 (2), 251–257.

Jackson, I.J., 1975. Relationships between rainfall parameters and interception by tropical forest. J. Hydrol. 24 (3–4), 215–238.

Jury, M.R., Raholijao, N., Nassor, A., 1995. Variability of summer rainfall over Madagascar: climatic determinants and interannual scales. Int. J. Climatol. 15 (12), 1323–1332.

Kijne, J.W., 1973. Determining evapotranspiration. In: de Ridder, N.A. (Ed.), Drainage Principals and Applications. Volume III. Surveys and Investigations. International Institute for Land Reclamation and Improvement, Wageningen, The Netherlands, pp. 53–111 (Chapter 19).

Lacombe, G., Ribolzi, O., de Rouw, A., Pierret, A., Latsachak, K., Silvera, N., Pham Dinh, R., Orange, D., Janeau, J.L., Soulileuth, B., Robain, H., Taccoen, A., Sengpaathith, P., Mouche, E., Sengtaheuanghoung, O., Tran Duc, T., Valentin, C., 2015. Afforestation by natural regeneration or by tree planting: examples of opposite hydrological impacts evidenced by long-term field monitoring in the humid tropics. Hydrol. Earth Syst. Sci. Discuss. 12, 12615–12648.

Lambin, E.F., Meyfroidt, P., 2010. Land use transitions: socio-ecological feedback *versus* socio-economic change. Land Use Policy 27, 108–118.

Lawrence, D., Radel, C., Tully, K., Schmook, B., Schneide, L., 2010. Untangling a decline in tropical forest resilience: constraints on the sustainability of shifting cultivation across the globe. Biotropica 42 (1), 21–30.

Levia, D.F., Germer, S., 2015. A review of stemflow generation dynamics and stemflow-environment interactions in forests and shrublands. Rev. Geophys. 53 (3), 673–714.

Levia, D.F., Herwitz, S.R., 2005. Interspecific variation of bark water storage capacity of three deciduous tree species in relation to stemflow yield and solute flux to forest soils. Catena 64 (1), 117–137.

Lloyd, C.R., 1990. The temporal distribution of Amazonian rainfall and its implications for forest interception. Quart. J. Roy. Meteorol. Soc. 116 (496), 1487–1494.

Lloyd, C.R., de Marques-Filho, A.O., 1988. Spatial variability of throughfall and stemflow measurements in Amazonian rainforest. Agric. For. Meteorol. 42 (1), 63–73.

Lloyd, C.R., Gash, J.H.C., Shuttleworth, W.J., de Marques-Filho, A.O., 1988. The measurement and modelling of rainfall interception by Amazonian rain forest. Agric. For. Meteorol. 43 (3–4), 469–485.

Macinnis-Ng, C.M.O., Flores, E.E., Müller, H., Schwendenmann, L., 2012. Rainfall partitioning into throughfall and stemflow and associated nutrient fluxes: land-use impacts in a lower montane tropical region of Panama. Biogeochemistry 111, 661–667.

Macinnis-Ng, C.M.O., Flores, E.E., Müller, H., Schwendenmann, L., 2014. Throughfall and stemflow vary seasonally in different land-use types in a lower montane tropical region of Panama. Hydrol. Process. 28 (4), 2174–2184.

Manfroi, O.J., Koichiro, K., Nobuaki, T., Masakazu, S., Nakagawa, M., Nakashizuka, T., Chong, L., 2004. The stemflow of trees in a Bornean lowland tropical forest. Hydrol. Process. 18 (13), 2455–2474.

Marquardt, D.W., 1963. An algorithm for least-square estimates of nonlinear parameters. J. Soc. Ind. Appl. Math. 11, 431–441.

Météo Madagascar, 2013. Precipitation data CAZ 1983-2013. Technical report, Météo Madagascar, Ministère des Transports et de la Météorologie, Antananarive.

Miralles, D.G., Gash, J.H., Holmes, T.R.H., de Jeu, R.A.M., Dolman, A.J., 2010. Global canopy interception from satellite observations. J. Geophys. Res. 115, D16122.

Monteith, J.L., 1965. Evaporation and the environment. In: 19th Symposium of the Society for Experimental Biology, vol. 19, pp. 205–234.

Mukul, S.A., Herbohn, J., 2016. The impacts of shifting cultivation on secondary forest dynamics in the tropics: a synthesis of the key findings and spatio-temporal distribution of research. Environ. Sci. Policy 55, 167–177.

Mukul, S.A., Herbohn, J., Firn, J., 2016. Tropical secondary forests regenerating after shifting cultivation in the Philippines uplands are important carbon sinks. Sci. Rep. 6, 22483. http://dx.doi.org/10.1038/srep22483.

Murakami, S., 2009. Abrupt changes in annual stemflow with growth in a young stand of Japanese cypress. Hydrol. Res. Lett. 3, 32–35.
Nash, J.E., Sutcliffe, J.V., 1970. River flow forecasting through conceptual models. Part I – A discussion of principles. J. Hydrol. 10 (3), 282–290.
Nespor, V., Sevruk, B., 1999. Estimation of wind-induced error of rainfall gauge measurements using a numerical simulation. J. Atmos. Ocean. Technol. 16, 450–464.
Ogden, F.L., Crouch, T.D., Stallard, R.F., Hall, J.S., 2013. Effect of land cover and use on dry season river runoff, runoff efficiency, and peak storm runoff in the seasonal tropics of Central Panama. Water Resour. Res. 49 (12), 8443–8462.
Oguntoyinbo, J.S., 1970. Reflection coefficient of natural vegetation, crops and urban surfaces in Nigeria. Quart. J. Roy. Meteorol. Soc. 96 (409), 430–441.
Pereira, F.L., Valente, F., Davis, J.S., Jackson, N., Minunno, F., Gash, J.H., 2016. Rainfall interception modelling: is the wet bulb approach adequate to estimate mean evaporation rate from wet/saturated canopies in all forest types? J. Hydrol. 534, 606–615.
Portela, R., Nunes, P., Onofri, L., Villa, F., Shepard, A., Lange, G., 2012. Assessing and valuing ecosystem services in the Ankeniheny-Zahamena corridor. In: Madagascar: a Demonstration Case Study for the Wealth Accounting and the Valuation of Ecosystem Services (WAVES) Global Partnership, pp. 56.
Riehl, H., 1979. Climate and Weather in the Tropics. Academic Press, New work, p. 611.
Roberts, J.M., Gash, J.H.C., Tani, M., Bruijnzeel, L.A., 2005. Controls on evaporation in lowland tropical rainforest. In: Bonell, M., Bruijnzeel, L.A. (Eds.), Forests, Water and People in the Humid Tropics. Cambridge University Press, Cambridge, UK, pp. 622–650.
Scatena, F.N., Bruijnzeel, L.A., Bubb, P., Das, S., 2010. Setting the stage. In: Bruijnzeel, L.A., Scatena, F.N., Hamilton, L.S. (Eds.), Tropical Montane Cloud Forests. Science for Conservation and Management. Cambridge University Press, Cambridge, UK, pp. 3–13.
Schellekens, J., Scatena, F.N., Bruijnzeel, L.A., Wickel, A.J., 1999. Modelling rainfall interception by a lowland tropical rainforest in northeastern Puerto Rico. J. Hydrol. 225 (3–4), 168–184.
Schrott, G., Fereira da Silva, L., Wolf, W.A., Texeira, W.G., Zech, W., 1999. Distribution of throughfall and stemflow in multi-strata agroforestry, perennial monoculture, fallow and primary forest in Central Amazonia, Brazil. Hydrol. Process. 13, 1423–1436.
Styger, E., Rakotondramasy, H.M., Pfeffer, M.J., Fernandes, E.C.M., Bates, D., 2007. Influence of slash-and-burn farming practices on fallow succession and land degradation in the rainforest region of Madagascar. Agric. Ecosyst. Environ. 119 (3–4), 257–269.
Swank, W.T., Vose, J.M., Elliott, K.E., 2001. Long-term hydrologic and water quality responses following commercial clearcutting of mixed hardwoods on a Southern Appalachian catchment. For. Ecol. Manage. 143 (1–3), 163–178.
Tadross, M., Randriamarolaza, L., Rabefitia, Z., Yip, Z., 2008. Climate change in Madagascar; recent, past and future. Technical report, Climate Systems Analysis Group, University of Cape Town, South Africa, and National Meteorological Office, Antananarivo, 17 pp.
Thom, A.S., 1975. Momentum, mass, and heat exchange of plant communities. In: Monteith, J.L. (Ed.), Vegetation and the Atmosphere, 1. Principles. Academic Press, London, UK, pp. 57–109.
Ubarana, V.N., 1996. Observations and modelling of rainfall interception at two experimental sites in Amazonia. In: Gash, J.H.C., Nobre, C.A., Roberts, J.M., Victoria, R.L. (Eds.), Amazonian Deforestation and Climate. J. Wiley, Chichester, UK, pp. 151–162.
Van Dijk, A.I.J.M., Bruijnzeel, L.A., 2001a. Modelling rainfall interception by vegetation of variable density using an adapted analytical model. Part 1. Model description. J. Hydrol. 247 (3–4), 230–238.
Van Dijk, A.I.J.M., Bruijnzeel, L.A., 2001b. Modelling rainfall interception by vegetation of variable density using an adapted analytical model. Part 2. Model validation for a tropical upland mixed cropping system. J. Hydrol. 247 (3–4), 239–262.
Wallace, J.S., McJannet, D., 2008. Modelling interception in coastal and montane rainforests in northern Queensland, Australia. J. Hydrol. 348 (3–4), 480–495.
Wallace, J.S., McJannet, D., 2012. Climate change impacts on the water balance of coastal and montane rainforests in northern Queensland, Australia. J. Hydrol. 475, 84–96.
Wallace, J.S., Macfarlane, C., McJannet, D., Ellis, T., Grigg, A., van Dijk, A.I.J.M., 2013. Evaluation of forest interception estimation in the continental scale Australian Water Resources Assessment – Landscape (AWRA-L) model. J. Hydrol. 499, 210–223.
Wickel, A.J., 2004. Water and nutrient dynamics of a humid tropical agricultural watershed in Eastern Amazonia. Ecology and Development Series, vol. 21. Center for Development Research, University of Bonn, Germany, p. 122.
Zeng, N., Shuttleworth, J.W., Gash, J.H.C., 2000. Influence of temporal variability of rainfall interception loss. Part I. Point analysis. J. Hydrol. 228 (3–4), 228–241.
Ziegler, A.D., Fox, J.M., Xu, J., 2009a. The rubber juggernaut. Science 324, 1024–1025.
Ziegler, A.D., Bruun, T.B., Guardiola-Claramonte, M., Giambelluca, T.W., Lawrence, D., Thanh Lam, N., 2009b. Environmental consequences of the demise in swidden cultivation in montane mainland Southeast Asia: hydrology and geomorphology. Hum. Ecol. 37, 361–373.
Ziegler, A.D., Giambelluca, T.W., Plondke, D., Leisz, S., Tran, L.T., Fox, J., Nullet, M.A., Vogler, J.B., Truong, D.M., Vien, T.D., 2004. Hydrological consequences of landscape fragmentation in mountainous northern Vietnam: buffering of accelerated overland flow. J. Hydrol. 337 (1), 52–67.
Zimmermann, B., Elsenbeer, H., 2009. The near-surface hydrological consequences of disturbance and recovery: a simulation study. J. Hydrol. 364 (1–2), 115–127.
Zimmermann, B., Zimmermann, A., Scheckenbach, H.L., Schmid, T., Hall, J.S., van Breugel, M., 2013. Changes in rainfall interception along a secondary forest succession gradient in lowland Panama. Hydrol. Earth Syst. Sci. 17, 4659–4670.